Fast optical sampling by electronic repetition-rate tuning using a single mode-locked laser diode

Research Article Vol. 29, No. 5 / 1 March 2021 / Optics Express 6890
Optics EXPRESS

Fast optical sampling by electronic repetition-rate tuning using a single mode-locked laser diode

D. BAJEK[1,2] AND M. A. CATALUNA[1,3]

[1]School of Engineering and Physical Sciences, Heriot-Watt University, Edinburgh, EH14 4AS, United Kingdom
[2]d.bajek@hw.ac.uk
[3]m.cataluna@hw.ac.uk

Abstract: This paper demonstrates optical sampling by electronic repetition-rate tuning (OSBERT): a single-laser optical sampling technique capable of fast scan rates and customisable scan ranges. The method has no moving parts and is based on the electronic modulation of the repetition rate of a passively mode-locked laser diode, simply by varying the reverse bias applied directly to the saturable absorber section of the laser. Varying the repetition rate in a system built as a highly imbalanced interferometer results in pairs of (pump, probe) pulses with successive increasing delay. The resulting scan range is proportional to the magnitude of the repetition rate modulation and is scaled by the chosen length of the imbalance. As a first proof of concept, we apply the method to distance measurement, where the displacement of a target across 13.0 mm was detected with ~0.1 mm standard deviation from an equivalent free-space distance of 36 m and at a real-time scan rate of 1 kHz. The customizable scan range and competitive scan rate of the method paves the way for single ultrafast semiconductor laser diodes to be deployed as fast, low-cost, and compact optical sampling systems in metrology, biomedical microscopy, and sensing applications.

1. Introduction

1.1. Optical sampling

Applications for optical sampling techniques include imaging, sensing and communications across the fields of attoscience [1], femtochemistry [2], and life sciences [3]. The basis of optical sampling techniques such as those used in pump-probe spectroscopy is to provide some temporal delay between two ultrashort pulses: a high energy excitation pump pulse and a low energy probe pulse. The delay between these pulses may be varied, allowing events between successive pulses to be analyzed. The conventional approach to introduce and vary such optical delay between pulses is to use mechanical translation stages fitted with retroreflectors. Due to its mechanical nature, this approach is intrinsically limited in scan rate [4]. On the other hand, ASOPS – asynchronous optical sampling [5], achieves the delay between pump and probe pulses by instead adopting two pulsed lasers with a small difference in repetition rate f_{pump} and f_{probe} such that $\Delta f = f_{pump} - f_{probe}$. This fixed repetition-rate difference causes the pump and probe pulses to reach the target with a mutual delay which increases incrementally with each successive pair of pulses until a full roundtrip period $1 / f_{pump}$ has been scanned. This method improves upon the conventional delay stage mechanism firstly by having no mechanical parts, and secondly by an increase in potential scan rate, which is as high as the difference in repetition rate Δf - to date practically demonstrated at multiple kHz scan rates [6]. One of the limitations of ASOPS is that the scan range is fixed and dictated by $1 / f_{pump}$ [7] and scans must acquire this entire

#413045 https://doi.org/10.1364/OE.413045
Journal © 2021 Received 27 Oct 2020; revised 16 Dec 2020; accepted 16 Dec 2020; published 19 Feb 2021

Optics EXPRESS

temporal range which is often fairly long compared to typical ultrafast events which may occur over femtoseconds to picoseconds. Therefore, any scan range exceeding that which is required leads to dead time, and scans take disproportionately longer to complete than the event of interest. ECOPS – electronically controlled optical sampling [8], improves upon some of these drawbacks by modulating the repetition rate of one of the lasers, whilst the other laser is kept constant [9]. This allows a customizable scan range of interest within the round-trip period to be selected, reducing the dead time and potentially also increasing the scan rate. For example, ECOPS was recently used to demonstrate THz-based thickness measurements at 1600 scans per second over a 200 ps scan range [10]. Crucially, both ECOPS and ASOPS require two lasers, which doubles not only the costs and footprint of such systems, but significantly increases their complexity in matters of the hardware and software required in phase-locking both pulse trains accurately.

The OSCAT method – optical sampling by laser cavity tuning [11] – uses only one laser in combination with a highly imbalanced interferometer, where the pump pulses are sent to the target, and the probe pulses are delayed via a passive delay line (PDL) of length l and refractive index n. The delay line in this configuration is entirely stationary, with no mechanical delay stage, providing a spatial delay which is so long (accommodating many periods T of repetition rate f, where $T = 1/f$), that adjusting the repetition rate of the source laser from f to $f + \Delta f$ leads to a scan range $\Delta\tau$ given by

$$\Delta\tau = \frac{l \cdot n \cdot f}{c}\left(\frac{1}{f} - \frac{1}{f + \Delta f}\right) \tag{1}$$

where c is the speed of light in a vacuum. As the repetition rate value is incrementally increased from a minimum to a maximum across the tuning range (using a piezo stack to control the laser cavity length) the probe pulse is delayed temporally with respect to the pump pulse. Figure 1 shows the role the passive delay line plays in conjunction with the ability to vary the repetition rate.

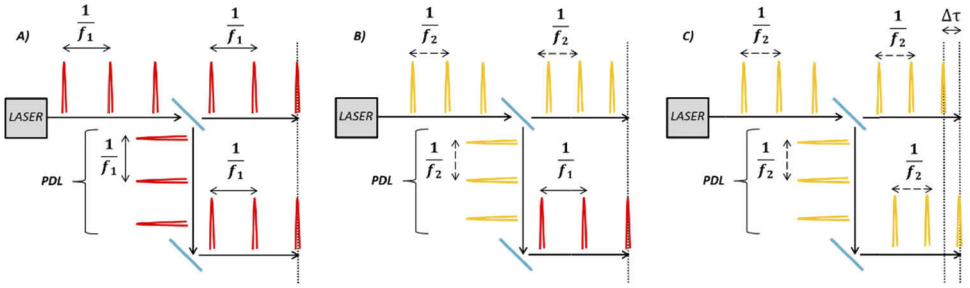

Fig. 1. Schematic diagram illustrating the general optical sampling principle of OSCAT. A) The initial repetition rate $f_1 = f$ propagates both the short and the long (PDL) arms, with no delay at the target position B) the laser's repetition rate is increased to $f_2 = f + \Delta f$, causing an increasing delay between pulse pairs, leading eventually to C) f_2 has now traversed the PDL resulting in a consistent delay between the pulses.

Whilst the OSCAT design is simpler than ASOPS or ECOPS, it still relies on a mechanically driven change in laser cavity length, meaning there remain certain limitations in the potential for scan rate. OSREFM – Optical Sampling by Repetition Frequency Modulation [12] – adopted the same OSCAT sampling principle illustrated in Fig. 1 and applied it in a configuration where the repetition rate of a gain-switched semiconductor laser diode was modulated. Although OSREFM was only demonstrated at lower scan rates of up to 333 Hz, this single-laser technique does remove the need for any mechanical parts, as the repetition rate is modulated directly via an electrical signal. It does, however, require complicated locking electronics to both set and lock the repetition rate and its modulation. Moreover, it was noted that the system exhibited a fairly

Optics EXPRESS

high pulse-to-pulse jitter of around 10 ps. The high jitter values were attributed to both the driving electronics and the gain switching mechanism itself, due to the influence of amplified spontaneous emission during the formation of the pulses.

In the realm of pulse generation from laser diodes, it is known from the literature that typically, ultrashort pulses emitted directly from gain-switched laser diodes display longer pulse durations and higher timing jitter values than mode-locked laser diodes [13]. This is significant, because as previously reported for OSCAT (and applicable to OSREFM), the pulse-to-pulse jitter of the laser used can have a very deleterious effect on the accuracy of the optical sampling method [14].

In order to overcome the need for mechanical repetition rate tuning used in OSCAT, this paper presents a new approach – OSBERT, optical sampling by electronic repetition-rate tuning [15]. An OSBERT setup begins with the basic principle of OSCAT (illustrated in Fig. 1): an imbalanced interferometer with a PDL so long that electronically varying the repetition rate of a mode-locked laser diode (MLLD) varies the delay between pump and probe pulses. Depending on the application, either the PDL length l or the range of repetition rate tunability Δf may be adjusted to optimise the available scan range $\Delta\tau$ according to Eq. (1). Moreover, unlike OSREFM, OSBERT does not use gain-switched laser diodes, but instead makes use of the possibility of dynamic biasing of mode-locked laser diodes and consequent repetition rate tuning, as will be described in the next section.

1.2. Mode-locked laser diodes

Mode-locked laser diodes are low-cost, compact lasers which, depending on their fabrication, composition and structure, may generate pulses across a wide variety of repetition rates, wavelengths, pulse durations, and optical powers [16–18]. With MLLDs, passive mode-locking can be easily implemented with a two-section laser diode, such as the one represented schematically in Fig. 2. In these lasers, whilst the gain section is forward biased, a saturable absorber section is simultaneously reverse biased until the gain and loss dynamics of each section leads to passive mode-locking and the generation of ultrashort pulses.

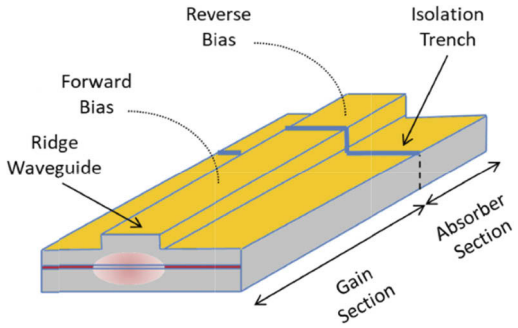

Fig. 2. Diagram of a typical MLLD with a reverse biased saturable absorber section which is electrically isolated from a forward biased gain section.

An intriguing aspect of MLLDs is the ability to tune their repetition rate entirely electronically by varying the diode-driving conditions without the need for a tunable external cavity; this has been demonstrated by varying combinations of the device's temperature, gain current or absorber bias [19–21]. OSBERT makes use of this versatility in order to generate a variable repetition rate controlled electronically via the reverse bias applied to the saturable absorber, resulting in an optical sampling scheme without any moving parts.

The possible mechanisms that underlie the electronic repetition rate tunability in these lasers have been widely discussed in the literature. This is due to greatly varying trends in tunability between device structures, compositions and characteristics. One such explanation relies on the

Optics EXPRESS

Pockels' effect, where the application of an electrical field across either section of the device may lead to variations in its refractive index, often indicated by observed variations in the central emission wavelength [20]. Similarly, the plasma effect has been cited as a potential cause [22,23], where a change in the refractive index is induced by a change in carrier density [24] during biasing. Another possible contributor may be the quantum confined Stark effect [25,26], which describes the effect of an external electric field upon the light absorption spectrum or emission spectrum of quantum-confined materials such as quantum wells or quantum dots. In the absence of an external electric field, electrons and holes within the quantum confined structure may only occupy states within a discrete set of energy sub-bands or levels. Consequently, only a discrete set of frequencies of light may be absorbed or emitted by the system. When an external electric field is applied, the electron states shift to lower energies, while the hole states shift to higher energies. This reduces the permitted light absorption or emission frequencies, and as such the wavelength of light generated may change slightly due to changes in biasing conditions [27,28]. Given that the refractive index of MLLDs is by extension wavelength-dependent, this could in turn slightly vary the propagation speed, and thus, the pulse repetition rate. Finally, repetition rate tuning has also been attributed to 'detuning time': temporal shifts in the pulse position through reshaping within the biased absorber and gain sections, which cause the repetition rate to deviate from the Fabry-Pérot round-trip time [20,21,29].

In addition to the versatility described above, it is important to note that not only do MLLDs typically display lower pulse-to-pulse jitter values than gain-switched lasers, but also that quantum-dot MLLDs have also demonstrated superior jitter performance over their quantum-well counterparts [16]. This is due to the reduced amplified spontaneous emission in quantum-dot materials (brought on by greater carrier confinement), which is one of the primary sources of jitter in passive mode-locked laser diodes [30,31]. We have therefore selected a quantum-dot MLLD to be at the core of this first demonstration of OSBERT. To prove the principle, we then carried out a distance measurement, as introduced in the following section.

1.3. Optical sampling for distance measurement

As a first proof of concept, the application tested in this paper is distance measurement [32–34]. OSCAT is regularly demonstrated to be an ideal tool for absolute distance measurement, particularly at long distances [32], where the long PDL intrinsically can be the distance to a stationary or moving target. LIDAR (light detection and ranging) was the tested application of Yang *et al.* [35], recording vibrations of a moving target as low as 15μm at several kilometres distance, at an update rate of 50Hz. Whilst kilometres-distances are impractical in the laboratory setting, in this case the PDL was a coiled optical fibre intended to represent the potential for long range distance measurement, and a moving retroreflecting mirror at the end of one of the arms was considered the target [35]. Facing the same practical limitations, we make these same mitigations in our following distance measurement experiments, as will be shown in the next section.

2. Experimental results

2.1. Experimental setup

Distance measurement through the generation of an interferometric cross-correlation at several different points is adopted as a first proof of principle for OSBERT. This was implemented using the experimental setup illustrated in Fig. 3.

By cross-correlating pulses originating from each arm and moving the target to displace the cross-correlation signal, a distance between traces could be measured which were directly proportional to the distance moved. We therefore adopt a similar scenario to [35] described in the previous section, whereby the mirror mounted on the mechanical stage was considered a moving

Optics EXPRESS

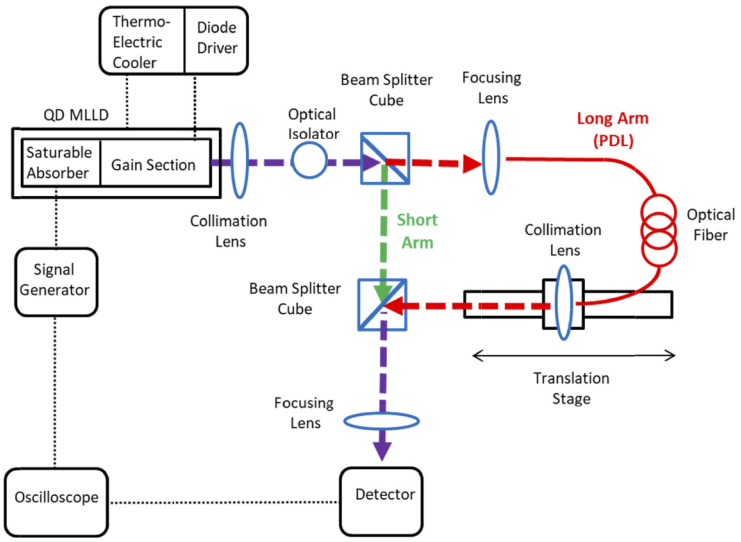

Fig. 3. The experimental setup allows for both a mechanical stage acquisition and an OSBERT acquisition of the same cross-correlation between one pulse propagating in the short arm and another propagating in the long arm of an interferometer.

target situated some distance away; in this case we make use of the long PDL arm to serve as this effective distance. However, instead of moving the mirror (which in our case is the beam-splitter cube) we move the fiber-launch system as a reciprocal analogue. The optical fiber serving as the PDL is mounted with a collimation lens on the translation stage, making this the target within the optical sampling setup whose position is altered and measured.

In order to achieve fast scanning using the highly imbalanced interferometer setup of OSBERT, we must modulate the bias to the absorber section of the MLLD in order to modulate the repetition rate by Δf, which combined with the imbalance in length of PDL will give rise to a scan range $\Delta\tau$. The absorber bias modulation is achieved using a signal generator (Keysight Technologies 33612A Waveform Generator, 80MHz). The two pulse trains then recombine at a detector (Thorlabs InGaAs DET08CL/M, 5GHz bandwidth), whose output signal is received at an oscilloscope (Teledyne Lecroy HDO4104, 1GHz bandwidth).

As a central component of OSBERT, we now turn our attention to the MLLD used in the setup. With reference to Fig. 2, the InGaAs-based quantum-dot narrow-ridged waveguide device was fabricated with a total length of 8.00 mm corresponding to a repetition rate of approximately 5 GHz. The total absorber length was 900 μm, while the narrow ridge waveguide was 4 μm wide. The absorber and gain sections were electrically isolated from each other via isolation trenches. The back facet was highly reflective while the front facet had a low-reflectivity coating.

In order to ascertain the parameters of operation of the laser which would enable OSBERT, an extensive characterisation of its performance was carried out. For this work, typical device output characteristics under a forward bias of 210 mA applied to the gain section and a reverse bias of 4.60 V applied to the absorber section are: a repetition rate of 5.079 GHz, pulse duration of approximately 5 ps, average power of approximately 6 mW, optical peak power of approximately 215 mW and an optical spectrum centred at ~1265 nm. Importantly, the greatest repetition rate tunability Δf was found when the reverse bias to the saturable absorber was increased from 4.60 V to 7.80 V. The radio frequency (RF) spectra indicating the resultant repetition rates for this reverse bias range were analyzed, where in each case the position of their peak was extracted from a Lorentzian fit. As such, a total repetition rate tunability of $\Delta f \sim 10MHz$ is found for an

Optics EXPRESS

approximately linear change in reverse bias voltage to the absorber section of $\Delta V = 3.20V$. The resulting tuning range and an exemplar RF spectrum are depicted in Fig. 4.

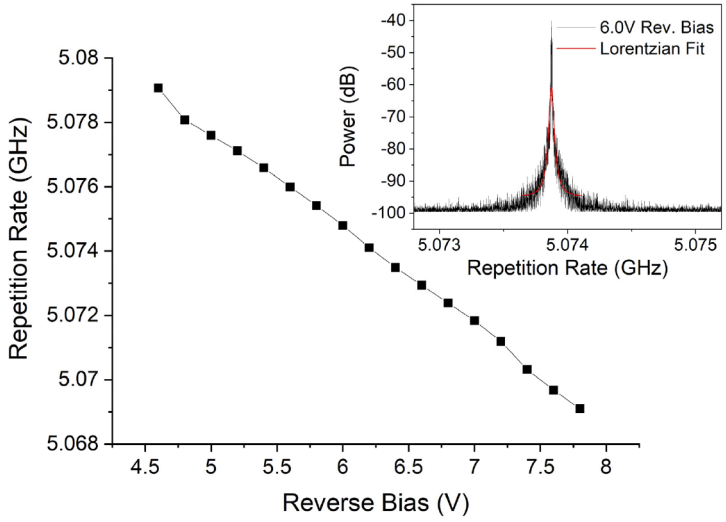

Fig. 4. Pulse repetition rate at 210 mA forward current to the gain section for increasing reverse bias to the absorber section. Inset: an example RF spectrum taken at 6.0 V reverse bias is fit with a Lorentzian function in order to determine the central frequency of the spectrum.

2.2. Experimental procedure

Prior to an OSBERT scan we firstly acquire a cross-correlation trace using the conventional mechanical delay-stage setup. The pulses propagating through the imbalanced arms of the interferometer are combined via the beam-splitter cube and directed towards the photodetector. The pulses of the long arm are temporally delayed with respect to those of the short arm by varying the position of the mechanical translation stage (Thorlabs LTS 300 mm), whilst acquiring the detector's signal at each position.

With the setup in place, an OSBERT scan of a cross-correlation may then be acquired, whereby the scan range $\Delta\tau$ is determined by Eq. (1), where the length l of the PDL is comprised of a 5 m optical fibre of refractive index $n = 1.46$, the fundamental repetition rate f is 5.079GHz and the repetition rate tunability Δf can be up to 10MHz. For an optical fibre PDL of length 5 m, this gives a scan range of 47.82 ps. As such, instead of moving the mechanical stage by a proportional distance and collecting a data point from the detector at each position, we hold the mechanical stage stationary, centralised at the peak position of a cross-correlation, and simply sweep the reverse bias to the absorber, detuning the resultant repetition rate, and generate a cross-correlation scan.

2.3. Mechanical scan vs OSBERT

The comparison mechanical stage cross correlation trace was acquired after applying the 210mA forward current to the gain section of the narrow-ridge device, and a mid-range 5.90V reverse bias to the absorber section in order to produce a stable picosecond pulse train. Mechanically sweeping the stage position generated the reference cross-correlation scan, as represented in Fig. 5. The spatial resolution in the mechanical stage trace is dictated by the step chosen for the incremental movement of the translation stage (in this case, 1 μm), and the acquisition time required for the full measurement was 322s.

Optics EXPRESS

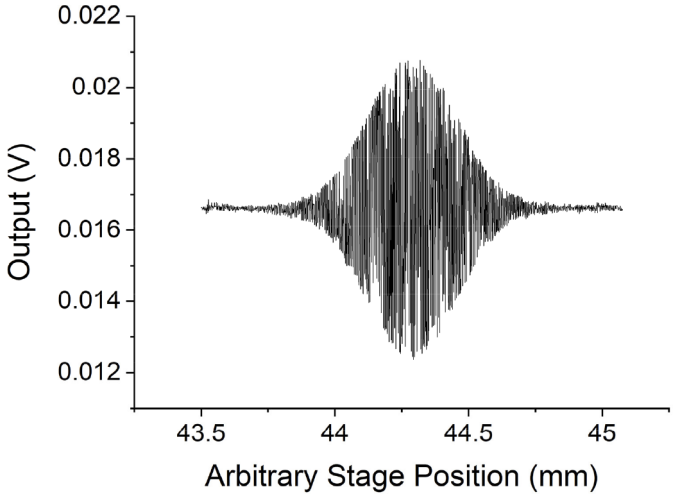

Fig. 5. Conventional mechanical stage cross-correlation trace across an arbitrary distance is taken at 210 mA forward current to the gain section and 5.90 V reverse bias to the absorber section. The central peak occurs at the stage position of 44.25 mm.

Noting the central position of the trace, we demonstrate OSBERT in Fig. 6 at a 1-kHz scan rate (the frequency of the sinusoidal modulation of the reverse bias) using the 5m length of optical fiber of refractive index 1.46 as a PDL, and a reverse bias modulation equivalent to Δf ~3.39 MHz repetition rate tuning, giving rise to a scan range which is sufficient to fully capture a cross-correlation event. Two periods of scanning are acquired on the time-base of the oscilloscope, therefore the acquisition time of one cross-correlation trace is 500μs, see Fig. 6.

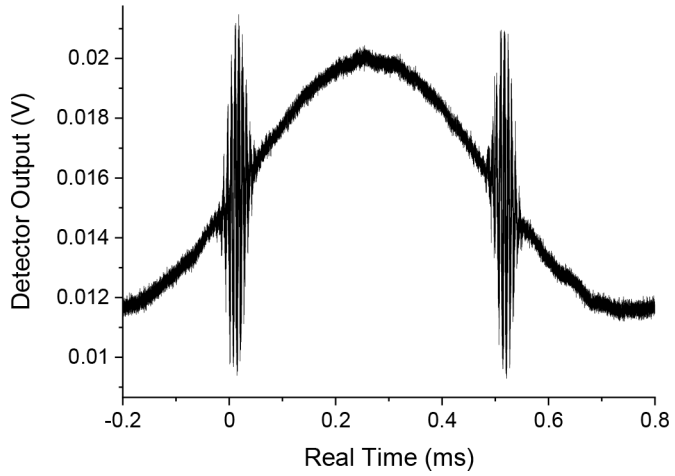

Fig. 6. 1 kHz OSBERT scans are shown within a real oscilloscope time-base of 1 ms.

In OSBERT, the spatial resolution mostly stems from the convolution of temporal step size between the pulses emerging from the two interferometer arms with the interferometric cross-correlation function, the number of pairs of pulses interfering per cycle, the electrical bandwidth of the detector (5 GHz), as well as the bandwidth of the oscilloscope (1 GHz) and its sampling rate (2.5 GSa/s maximum – corresponding to a sampling period T_s of 400ps).

Optics EXPRESS

For the setup conditions presented in the manuscript, the laser pulse repetition rate is ~5 GHz corresponding to a period of ~200 ps. Each pair of interfering pulses contributes to the cross-correlation signal. However, the oscilloscope sampling period is 400 ps. This can equally be converted to the spatial domain Δl_s (in mm) using $\Delta l_s = c \cdot T_s/1000$, leading to 0.12 μm minimum spatial step size (or resolution).

What is notable between these real-time scans and the mechanical counterparts is a reduction in the number of fringes detected, owed to the effects of aliasing; the faster scan rate means that the sharp temporal features of each fringe (that is, the rise time associate with one fringe) may be less clearly detectable by the 1 GHz bandwidth limit of the oscilloscope. Faster detection equipment, and / or slower scan rates would reduce this effect, depending on the detail required for the chosen application.

2.4. Distance measurements using OSBERT

For distance measurement, we select a longer optical fiber PDL length of 25 m (refractive index 1.46) is selected for the long arm, providing a target distance of 36 m in equivalent free-space, and the repetition rate tunability is set to ~3.39 MHz via appropriate sinusoidal modulation of the reverse bias applied to the absorber section, ultimately corresponding to a total available scan range $\Delta\tau$ of 81.3 picoseconds (or 24.4 millimeters in the spatial domain Δl) – as theorized above, this longer PDL has given rise to a longer (customizable) scan range than that given by the 5m optical fiber described above. The target is moved from its origin to various positions with the mechanical translation stage, whilst simultaneously running the OSBERT scanner at a 1kHz scan rate. At each 1.0 mm change in the target position, an OSBERT cross-correlation is acquired and superimposed on the predecessor scan. Thirteen consecutive target position traces were acquired, see Fig. 7.

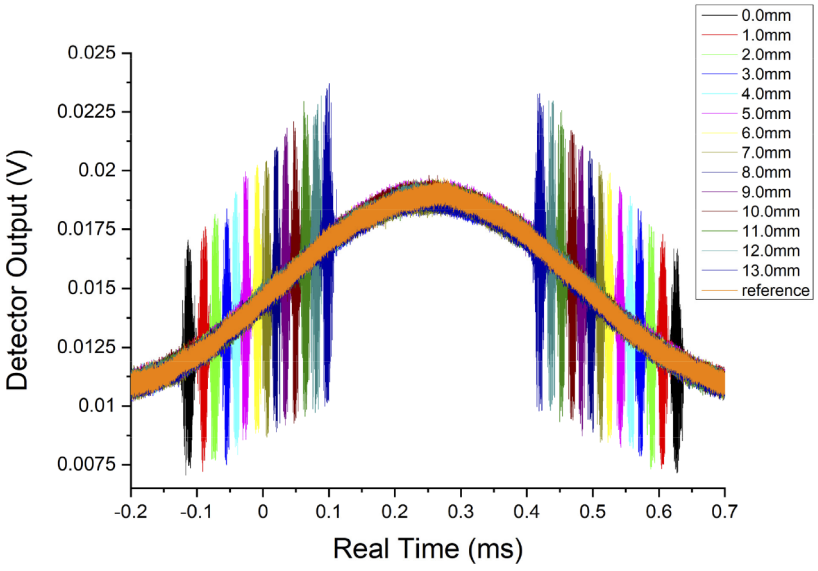

Fig. 7. Raw, real-time oscilloscope traces of 1 kHz OSBERT scans at several target positions.

These raw-data scans were acquired in-real time, where target motion was instantly detectable without the need for signal enhancement or improvement by averaging. In order to convert from the real time t of the oscilloscope trace to a repetitively scanned delay time $\Delta\tau(t)$, we adopt the

Optics EXPRESS

theory outlined in [35], which deconvolves the traces from sinusoidal form to linear form by

$$\tau(t) \approx \frac{\Delta f.T_0}{f} sin\left[2\pi f_m\left(t + \frac{T_0}{2}\right)\right] \tag{2}$$

where Δf is the repetition rate tunability, T_0 is the passive delay time corresponding to a PDL of length l such that $T_0 = ln/c$ (where n is the refractive index of the PDL), f is the fundamental repetition rate and f_m is the frequency of sinusoidal modulation of the change in repetition rate (i.e., the scan rate). Subtracting a reference baseline scan, and applying this function to the real-time axis t represents the scans in terms of the scan range $\Delta\tau$, which may then be converted to the spatial domain Δl in millimeters using $\Delta l = c \cdot \Delta\tau/1000$, we now have a representation of each acquisition at the target position, see Fig. 8.

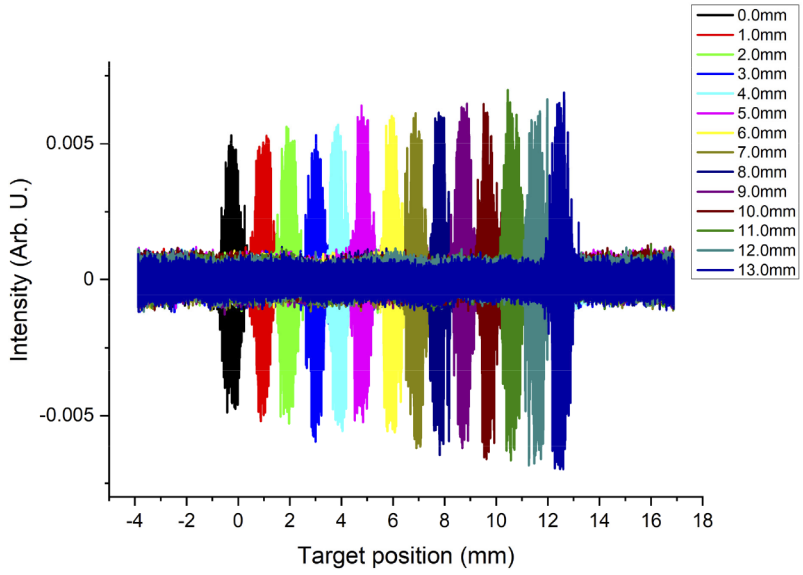

Fig. 8. 1 kHz OSBERT scans converted from a real time axis to delay time, represented in the spatial domain.

The measured value of the position at each distance was extracted from the peak of the cross-correlation – an approach widely adopted in the field (for example, as shown in [32]). In order to do this, we fitted a Gaussian function to each cross-correlation trace shown in Fig. 8, and from this fit we extracted the fitted parameter corresponding to the abscissa of the peak of the Gaussian. For each distance, this parameter provides the measured distance moved and it is represented in Fig. 9 in comparison with the actual distance moved on the translation stage in 1 mm increments, where a 1:1 line serves to represent the accuracy of the measurements. The average (0.978 mm) and standard deviation (0.10 mm) of the expected 1.0 mm target motions was then calculated from this series.

Conceptually, this ultimately means we have detected millimeter to centimeter range movements of a target situated at an equivalent free-space distance of 36 meters from the OSBERT detector, to within 0.1 mm standard deviation, at a fast scan rate of 1kHz. According to the manufacturer's specifications, a maximum absolute accuracy of 0.07 mm may have been contributed by the translation stage used. While this is independent of any error present in the OSBERT system itself, it may have contributed to some extent to the accuracy of the distance measurement, as for each set position in the translation stage, there could be a slight difference between the commanded (ideal) position and the absolute position.

Optics EXPRESS

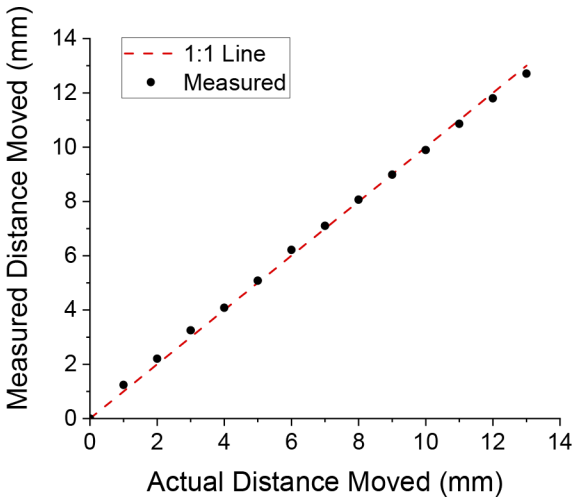

Fig. 9. Values of distance moved measured with OSBERT, as a function of the values of distance moved by the mechanical translation stage.

Given that OSBERT is presented here as a time-sensitive cross-correlation technique, we shall consider the pulse to pulse timing jitter σ_{pp} as a comparison with the OSREFM technique described above. Kefelian et al. [36] have shown that the pulse to pulse timing jitter may be extracted using the RF linewidth $\Delta\upsilon$ of the RF spectrum of central repetition rate frequency f_{rep} as a figure of merit for the magnitude of jitter, which is found to increase for the increasing number of periods N between pulses, such that $N = l \cdot n \cdot f_{rep}/c$ is the scaling factor of Eq. (1), and where

$$\sigma_{pp}(N) = \frac{1}{f_{rep}}\sqrt{\frac{\Delta\upsilon N}{2\pi f_{rep}}} \tag{3}$$

This is particularly relevant for OSBERT, where greater scan ranges may be brought about by increasing the PDL length l within the cross-correlator, and therefore increasing the number of roundtrip periods therein.

Using the Kefelian approach, RF spectra from Fig. 4 were fit with a Lorentzian function in order to determine their linewidth, which were around 15kHz. Substituting this into Eq. (3), we may calculate the jitter according to an increasing passive delay length. Firstly we note that for a 15kHz linewidth, the jitter associated with the MLLD alone (i.e., with just one period where $N = 1$) is 135 femtoseconds compared with the 10 picoseconds demonstrated by the GSLD used in OSREFM [12]. In conjunction with a PDL, the OSBERT system exhibits up to a maximum of 2.8 picoseconds of pulse to pulse timing jitter depending on the PDL length used (25 m in the case of this work). Due to the versatile nature of MLLD devices and the wide range of biasing conditions which may be utilised, the reverse bias used for scanning could be optimised for only those in the range of the lowest linewidth values. If a shorter PDL of just a few meters length and a smaller repetition rate tuning range Δf gives rise to a sufficient customisable scan range, conceivably pulse to pulse timing jitter as low as a few hundred femtoseconds could be present in the system.

We may now compare our results with some similar systems described above. Generally, there is a trade-off for scan rate and accuracy, where we have measured the movement of a target across 13.0 mm from an equivalent free-space distance of 36 m. At a scan rate of 1kHz we found agreement of the target motion with 0.1 mm standard deviation. An ASOPS setup presented in [37] detected the motion of optically rough objects from a distance of 0.5 m, with 10 μm

Optics EXPRESS

accuracy and at scan rates of 500 Hz. Terahertz impulse ranging [33] was used in a similar ASOPS arrangement at a scan rate of 10 Hz, and yielded an accuracy of −551 µm for target motions of 5 mm over a 200 mm range, from a scanning distance of 1 m. Similarly, an OSCAT arrangement was used for absolute distance measurement and found agreement within 10 µm from a target distance of 47 m [32].

Therefore, as well as improving the jitter, there are several other developments which will improve the quality and accuracy of the technique in the future. Since this work serves as a proof of concept, no signal processing was performed on the traces, such that they could be assessed in the context of live scanning, whereas most other techniques tend to time-average multiple traces in order to improve the signal to noise ratio and time-domain stability. Post-processing of the signal is also expected to improve the accuracy of metrology-related applications. Similar devices of differing semiconductor structures could also be fabricated and driven under optimised biasing conditions for reduced jitter, whilst a detection system with greater bandwidth could be used to improve how the traces are resolved at faster scan rates.

3. Conclusions

Optical sampling by repetition rate tuning (OSBERT) has been developed to take advantage of a number of the pros of the described techniques; namely the one-laser system of optical sampling by cavity tuning (OSCAT), the fast scan rates competitive with Electronically controlled optical sampling (ECOPS) and asynchronous optical sampling (ASOPS), and the optical sampling by repetition frequency modulation (OSREFM) premise of electronically varying the repetition rate of a laser diode, negating any need whatsoever for mechanical parts. The replacement of mechanical parts with an electronic change in reverse bias to the absorber section of the mode-locked laser diode (MLLD), provides a comparable cross-correlation trace to that of standard delay-stage methods. We then modulated the driving frequency of the scan and find repeatable acquisitions at up to kilohertz scan rates. Finally, as a proof of principle, we test the method on a distance measuring application, where the movement of a target across 13.0 mm was successfully measured at an equivalent free-space distance of 36 meters at a scan rate of 1kHz, with 0.1 mm standard deviation. Preliminary tests indicate that with further work, broader bandwidth detection equipment and some amount of signal processing, longer distances may be accurately measured at faster scan-rates approaching 10's to 100's of kHz, which would require increasing the modulation speed of the electrical bias signal to the absorber section of the MLLD.

Funding. Leverhulme Trust (PLP 2011-172); Engineering and Physical Sciences Research Council; H2020 European Research Council (640537).

Acknowledgments. The authors would like to thank Innolume GmbH (Germany) for the growth and fabrication of the mode-locked laser.

Disclosures. The authors declare no conflicts of interest.

References

1. P. B. Corkum and F. Krausz, "Attosecond science," Nat. Phys. **3**(6), 381–387 (2007).
2. A. H. Zewail, "Laser femtochemistry," Science **242**(4886), 1645–1653 (1988).
3. T. E. Matthews, J. W. Wilson, S. Degan, M. J. Simpson, J. Y. Jin, J. Y. Zhang, and W. S. Warren, "In vivo and ex vivo epi-mode pump-probe imaging of melanin and microvasculature," Biomed. Opt. Express **2**(6), 1576–1583 (2011).
4. K. F. Kwong, D. Yankelevich, K. C. Chu, J. P. Heritage, and A. Dienes, "400-Hz mechanical scanning optical delay line," Opt. Lett. **18**(7), 558–560 (1993).
5. P. A. Elzinga, F. E. Lytle, Y. Jian, G. B. King, and N. M. Laurendeau, "Pump/Probe Spectroscopy by Asynchronous Optical Sampling," Appl. Opt. **26**(19), 4303–4309 (1987).
6. A. Bartels, F. Hudert, C. Janke, T. Dekorsy, and K. Köhler, "Femtosecond time-resolved optical pump-probe spectroscopy at kilohertz-scan-rates over nanosecond-time-delays without mechanical delay line," Appl. Phys. Lett. **88**(4), 041117 (2006).
7. J. Jiang and A. Abuduweili, "High Resolution Measurement with Asynchronous Optical Sampling," in *Journal of Physics: Conference Series*, 2019.

Optics EXPRESS

8. F. Tauser, C. Rausch, J. H. Posthumus, and F. Lison, "Electronically controlled optical sampling using 100 MHz repetition rate fiber lasers," in *Commercial and Biomedical Applications of Ultrafast Lasers VIII*. 2008. United States: Proceedings of SPIE - The International Society for Optical Engineering: San Jose, CA.
9. D. S. Yee and Y. Kim, "High-speed terahertz time-domain spectroscopy based on electronically controlled optical sampling," Opt. Lett. **35**(22), 3715–3717 (2010).
10. M. Yahyapour, A. Jahn, K. Dutzi, T. Puppe, P. Leisching, B. Schmauss, N. Vieweg, and A. Deninger, "Fastest Thickness Measurements with a Terahertz Time-Domain System Based on Electronically Controlled Optical Sampling. Applied Sciences (Switzerland), 2019. 9.
11. T. Hochrein, R. Wilk, M. Mei, R. Holzwarth, N. Krumbholz, and M. Koch, "Optical sampling by laser cavity tuning," Opt. Express **18**(2), 1613–1617 (2010).
12. T. Furuya, E. S. Estacio, K. Horita, C. T. Que, K. Yamamoto, F. Miyamaru, S. Nishizawa, and M. Tani, "Fast-Scan Terahertz Time Domain Spectrometer Based on Laser Repetition Frequency Modulation," Jpn. J. Appl. Phys. **52**(2R), 022401 (2013).
13. P. Vasil'ev, *Ultrafast Diode Lasers: Fundamentals and Applications* 1995: Artech House Publishers
14. R. Wilk, T. Hochrein, M. Koch, M. Mei, and R. Holzwarth, "OSCAT: Novel Technique for Time-Resolved Experiments Without Moveable Optical Delay Lines," J. Infrared, Millimeter, Terahertz Waves **32**(5), 596–602 (2011).
15. D. Bajek, "High-Speed Optical Sampling Techniques Enabled By Ultrafast Semiconductor Lasers, in *Ch. 4*. 2016, University of Dundee.
16. M. G. Thompson, M. X. A. R. Rae, R. V. Penty, and I. H. White, "InGaAs Quantum-Dot Mode-Locked Laser Diodes," IEEE J. Select. Topics Quantum Electron. **15**(3), 661–672 (2009).
17. M. F. Li, H. Q. Ni, Y. Ding, D. Bajek, L. Kong, A. Cataluna Maria, and Z. C. Niu, "Optimization of InAs/GaAs quantum-dot structures and application to 1.3-μm mode-locked laser diodes," Chin. Phys. B **23**(2), 027803 (2014).
18. H. Wang, L. Kong, A. Forrest, D. Bajek, S. E. Haggett, X. Wang, B. Cui, J. Pan, Y. Ding, and M. A. Cataluna, "Ultrashort pulse generation by semiconductor mode-locked lasers at 760 nm," Opt. Express **22**(21), 25940–25946 (2014).
19. F. Camacho, E. A. Avrutin, A. C. Bryce, and J. H. Marsh, "Modelocking frequency tunability and timing jitter in an extended cavity mode-locked semiconductor laser," in *Lasers and Electro-Optics Society Annual Meeting, 1997. LEOS '97 10th Annual Meeting. Conference Proceedings.*, IEEE. 1997.
20. S. Arahira and Y. Ogawa, "Repetition-frequency tuning of monolithic passively mode-locked semiconductor lasers with integrated extended cavities. Quantum Electronics," IEEE J. Quantum Electron. **33**(2), 255–264 (1997).
21. E. Sooudi, S. Sygletos, A. D. Ellis, G. Huyet, J. G. McInerney, F. Lelarge, K. Merghem, R. Rosales, A. Martinez, A. Ramdane, and S. P. Hegarty, "Optical Frequency Comb Generation Using Dual-Mode Injection-Locking of Quantum-Dash Mode-Locked Lasers: Properties and Applications. Quantum Electronics," IEEE J. Quantum Electron. **48**(10), 1327–1338 (2012).
22. H. C. Cheng and C. P. Lee, "Investigation of quantum dot passively mode-locked lasers with excited-state transition," Opt. Express **21**(22), 26113–26122 (2013).
23. H. F. Liu, S. Arahira, T. Kunii, and Y. Ogawa, "Frequency-tunable millimetre-wave signal generation using a monolithic passively mode-locked semiconductor laser," Electron. Lett. **32**(8), 740–741 (1996).
24. S. Murata, A. Tomita, and A. Suzuki, "Influence of free carrier plasma effect on carrier-induced refractive index change for quantum-well lasers," IEEE Photonics Technol. Lett. **5**(1), 16–19 (1993).
25. D. A. B. Miller, D. S. Chemla, T. C. Damen, T. H. Wood, C. A. Burrus, A. C. Gossard, and W. Wiegmann, "Band-edge electroabsorption in quantum well structures - The quantum-confined Stark effect," Phys. Rev. Lett. **53**(22), 2173–2176 (1984).
26. X. Huang, A. Stintz, H. Li, A. Rice, G. T. Liu, L. F. Lester, J. Cheng, and K. J. Malloy, "Bistable operation of a two-section 1.3 μm InAs quantum dot laser-absorption saturation and the quantum confined Stark effect. Quantum Electronics," IEEE J. Quantum Electron. **37**(3), 414–417 (2001).
27. D. Kunimatsu, S. Arahira, Y. Kato, and Y. Ogawa, "Passively mode-locked laser diodes with bandgap-wavelength detuned saturable absorbers," IEEE Photonics Technol. Lett. **11**(11), 1363–1365 (1999).
28. P. M. Stolarz, J. Javaloyes, G. Mezosi, L. Hou, C. N. Ironside, M. Sorel, A. C. Bryce, and S. Balle, "Spectral Dynamical Behavior in Passively Mode-Locked Semiconductor Lasers," IEEE Photonics J. **3**(6), 1067–1082 (2011).
29. M. G. Thompson, A. Rae, R. L. Sellin, C. Marinelli, R. V. Penty, I. H. White, A. R. Kovsh, S. S. Mikhrin, D. A. Livshits, and I. L. Krestnikov, "Subpicosecond high-power mode locking using flared waveguide monolithic quantum-dot lasers," Appl. Phys. Lett. **88**(13), 133119 (2006).
30. E. U. Rafailov, M. A. Cataluna, and E. A. Avrutin, *Ultrafast lasers based on quantum dot structures : physics and devices*. 2011, Wiley-VCH: Weinheim, Germany.
31. J. P. Tourrenc, S. O'Donoghue, M. T. Todaro, S. P. Hegarty, M. B. Flynn, G. Huyet, J. G. McInerney, L. O'Faolain, and T. F. Krauss, "Cross-Correlation Timing Jitter Measurement of High Power Passively Mode-Locked Two-Section Quantum-Dot Lasers," IEEE Photonics Technol. Lett. **18**(21), 2317–2319 (2006).
32. H. Wu, F. Zhang, T. Liu, F. Meng, J. Li, and X. Qu, "Absolute Distance Measurement Using Optical Sampling by Cavity Tuning," IEEE Photonics Technol. Lett. **28**(12), 1275–1278 (2016).
33. T. Yasui, Y. Kabetani, Y. Ohgi, S. Yokoyama, and T. Araki, "Absolute distance measurement of optically rough objects using asynchronous-optical-sampling terahertz impulse ranging," Appl. Opt. **49**(28), 5262–5270 (2010).

Optics EXPRESS

34. M. Cui, M. G. Zeitouny, N. Bhattacharya, S. A. van den Berg, H. P. Urbach, and J. J. M. Braat, "High-accuracy long-distance measurements in air with a frequency comb laser," Opt. Lett. **34**(13), 1982–1984 (2009).
35. L. Yang, J. Nie, and L. Duan, "Dynamic optical sampling by cavity tuning and its application in lidar," Opt. Express **21**(3), 3850–3860 (2013).
36. F. Kefelian, S. O'Donoghue, M. T. Todaro, J. G. McInerney, and G. Huyet, "RF Linewidth in Monolithic Passively Mode-Locked Semiconductor Laser," IEEE Photonics Technol. Lett. **20**(16), 1405–1407 (2008).
37. W. Li, X. Qu, X. Zhao, and F. Zhang, "Absolute distance measurement of rough surfaces using asynchronous optical sampling," Opt. Eng. **58**(09), 1 (2019).